

# Computational Methods for Amorphous Semiconductor Devices

Ember L. Sikorski<sup>a</sup>

<sup>a</sup>Boise State University

---

## Abstract

- DOS
  - structural modeling
- 

## 1. Introduction

1.1. Why model amorphous semiconductors?

1.2. How can we model amorphous semiconductors?

Computational modeling spans length scales from the order of meters, that we experience, to the order of Angstroms, that atoms experience. Due to this vast range of length scales, no one method can address all properties. Following, computational methods are broken down into four main categories (Figure 1): First principles or *ab initio*, molecular dynamics (MD), mesoscale methods such as Monte Carlo (MC), and continuum methods such as finite element analysis (FEA)[1].

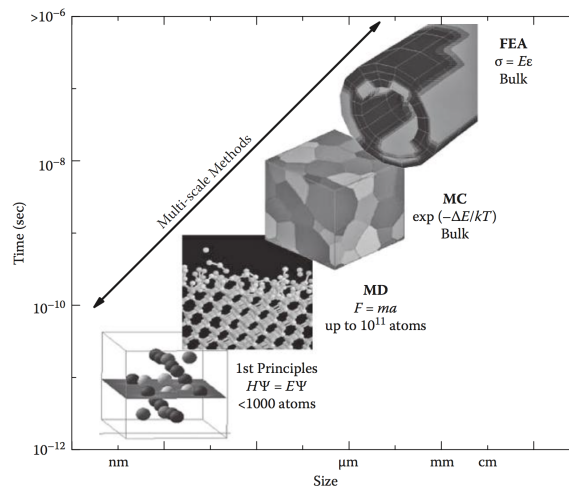


Figure 1: Overview of computational methods with respect to time and size capabilities. [1]

## 2. Methods

### 2.1. Field Theory

### 2.2. Monte Carlo

### 2.3. Molecular Dynamics

Molecular Dynamics (MD) is a classical method built off of

$$\vec{F} = m\vec{a} \quad . \quad (1)$$

Atoms are the smallest building block, represented as a sphere with a point mass [1]. To calculate desired properties, atoms are allowed to “relax” to their respective equilibrium distances, by moving down along the negative energy gradient:

$$\vec{F} = -\nabla U \quad . \quad (2)$$

A calculation begins with a set of starting atomic coordinates. The energy is calculated and the atoms are adjusted, following the gradient, to a more stable position. The energy is again calculated and compared to the previous step. This process continues until the differences between subsequent energy values reaches a predetermined stopping value, e.g. a difference of  $1 \times 10^{-4}$  eV or less.

This method requires selection of so-called pair-potentials, which describe how atom  $i$  interacts with atom  $j$ . The simplest potential is the Lennard-Jones potential:

$$U_{ij}(r) = 4\epsilon \left[ \left( \frac{\sigma}{r} \right)^{12} - \left( \frac{\sigma}{r} \right)^6 \right] \quad , \quad (3)$$

where  $\epsilon$  is the depth of the energy well and  $\sigma$  is the interatomic distance at which the potential is zero. However, this potential can only describe the interactions between atoms of the same element. In order to perform calculations on the majority of systems of interest, more complex pair-potentials are needed. Numerous potentials have been created, such as Embedded Atom Method (EAM) potentials which work for many metals and Tersoff potentials for covalent solids.

An alternative method necessary for our discussion of AIMD in Section YYY is the Lagrangian:

$$L = K - U = \frac{1}{2} \sum_{i=1}^{3N} m_i v_i^2 - U(r_1, \dots, r_{3N}) \quad , \quad (4)$$

where  $K$  is the kinetic energy,  $U$  is the potential energy, and  $N$  is the number of atoms.

### 2.4. Density Functional Theory

$$\hat{H} = -\frac{1}{2} \sum_i^n \nabla_i^2 - \sum_I^N \sum_i^n \frac{Z_I}{|r_{Ii}|} + \sum_{i \neq j}^n \frac{1}{|r_{ij}|} \quad (5)$$

$$\rho(r) = \sum_i |\phi_i(r)|^2 \quad (6)$$

## 2.5. Ab initio Molecular Dynamics

*Ab initio* Molecular Dynamics (AIMD) refers to any calculation that advances atoms along classical trajectories based on forces calculated from DFT[2].

AIMD is an incredibly powerful method capable of adding time to a DFT simulation while still allowing for *ab initio* calculation of electronic properties. Furthermore, AIMD can circumvent the problem of metastable states, as shown for DFT+U [3]. This can be better conceptualized with the schematic of Car-Parrinello MD in Figure YYY. Instead of performing AIMD as a stepwise process in which calculating the atomic trajectories and the electronic ground state are separate, Car and Parrinello formulated the two to run simultaneously. Their extended Lagrangian introduces the electronic degrees of freedom as fictitious dynamical variables:

$$L = \frac{1}{2} \sum_{i=1}^{3N} m_i v_i^2 - U(r_1, \dots, r_{3N}) + \frac{1}{2} \sum_j 2\mu \int d\vec{r} |\dot{\psi}(\vec{r})|^2 + L_{ortho} \quad (7)$$

The third term introduces fictitious mass,  $\mu$ , and the final term restrains the one-electron wave functions to be orthogonal. Since the total energy calculation occurs simultaneously with the atomic trajectory calculation, the energy is not quite the same as the energy calculated with pure DFT, as shown in Figure YYY. This phenomena circumvents the structure getting trapped in a metastable state, as DFT methods are known to do [4].

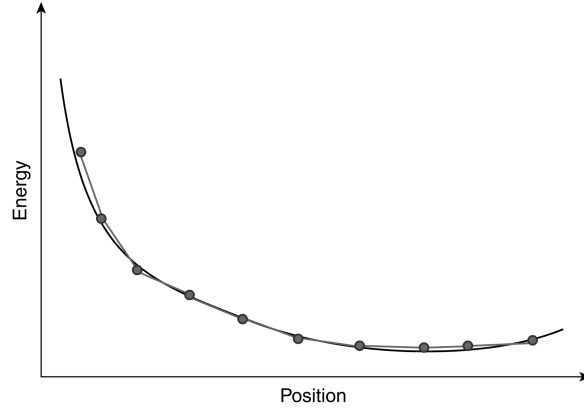


Figure 2:

### 2.5.1. AIMD for Phase Change Memory

Raty et al. [5] used Ab Initio Molecular Dynamics to understand the structural changes associated with aging in GeTe, and the effects those changes have on performance. Inherently out of equilibrium, amorphous materials evolve with time to a lower energetic state. In the case of phase change materials, this evolution leads to higher electrical resistivity that undermines its usability in multilevel memory devices. Using AIMD, we can watch the structure evolve, but though we discussed the addition of time to DFT above, this time is still on the order of picoseconds, leaving real-time aging out of the question. Raty et al. have sidestepped this problem by creating an arrangement of structures with varying local motifs.

Their study begins with the observation that AIMD simulations of  $\text{Ge}_x\text{Sb}_y\text{Te}_{1+x+y}$  alloys show tetrahedrally bonded Ge ( $\text{Ge}^T$ ) atoms in the amorphous phase, though these are absent in crystalline Ge. To investigate the effect of such homopolar bonds on GeTe properties, the authors melt-quenched GeTe along with a combination of other binary chalcogenides for use as “templates.” SiTe forms numerous  $\text{Si}^T$ , GeSe contains some  $\text{Ge}^T$ , and SnTe contains almost no tetrahedral motifs. The authors then substituted one species in each of the template compounds to form GeTe, i.e. substituting Si in SiTe with Ge, Se in GeSe with Te, and Sn in SnTe with Ge. After substitution, the systems were subjected to a shorter additional melt-quench procedure.

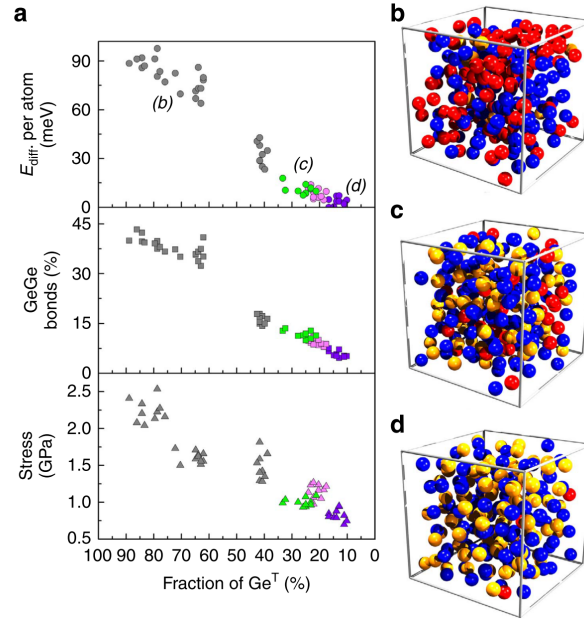


Figure 3: Results from Raty et al. [5] for (a) the energy difference per atom, fraction of homopolar GeGe bonds, and stress of the melt-quenching of GeTe (green) and chemical replacement systems SnTe (violet), GeSe (pink), and SiTe (grey). (b-d) show the atomic configurations of GeTe as labeled in the energy difference plot. Te, tetrahedral Ge, and octahedral Ge are rendered in blue, red, and orange, respectively.

The results shown in Figure. YYY indicate that the homopolar bonds reduce the stability of the system. However, homopolar bonds have a lower heat of formation in GeTe than in both GeSe and SnTe, and the melt-quench process is able to stabilize these tetrahedral motifs. In comparison to experiment, aging of phase change materials has been linked with stress relief. These results suggest that the removal of homopolar bonds contributes to this stress relief.

Raty et al. additionally calculated the changes in the electronic and optical bandgaps due to the changes in percent  $\text{Ge}^T$ . Though methods of calculating optical properties are beyond the scope of this review, the results of Raty et al. for the optical bandgap in Figures. YYY(a) and YYY show increasing band gap correlated with decreasing homopolar bonds, in agreement with experiment showing band gap widening with aging. Similarly, the DOS shows an increase in electronic band gap with aging, and the disappearance of the midgap states are directly linked to the removal of homopolar bonds. The authors note that while a variety of  $\text{Ge}^T$  concentrations have been modeled, this method does not yield access to the time scale of the relaxation process.

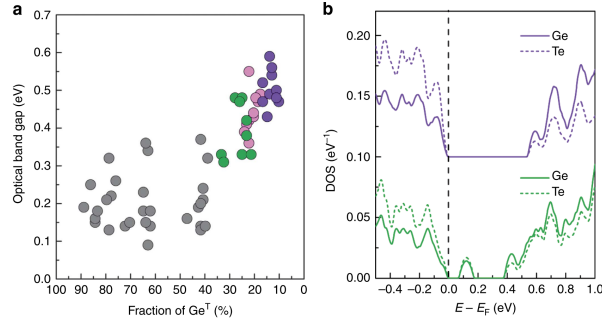


Figure 4: Results from Raty et al. [5] for (a) the relaxed amorphous GeTe structures as a function of percent  $\text{Ge}^T$  and (b) the local density of states for melt-quenched GeTe (green) and substituted a-SnTe (violet).

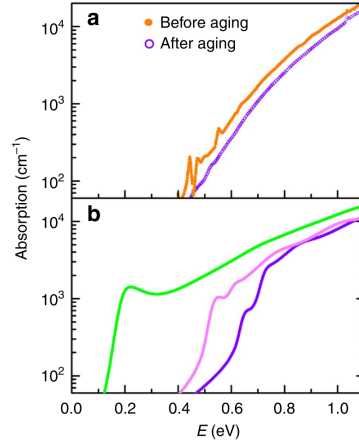


Figure 5: Results from Raty et al. [5] for (a) experimental absorption from photothermal deflection spectroscopy (PDS) and (b) calculated absorption oscillator strength for melt-quenched GeTe (green), substituted a-GeSe (pink), and substituted a-Sn-Te (violet).

### 2.5.2. Example AIMD melt-quench run

## Notes

- Kohn Sham: A *system* of one-electrons
- Hartree: a *potential* of how each electrons feels the electron gas
- Hartree Fock: how we describe the wave functions

### 2.6. AIMD

Hohl 1991[6] - Liquid and amorphous Se

#### Computational comments

- many structural models have been proposed and often conflict
- models based solely on small differences are insufficient to explain all measured features
- even carefully constructed empirical potentials have difficulty in highly anisotropic covalent systems such as group-IVA elements.
- AIMD avoids parameterization of interatomic forces common in MD

Raty 2015 [5] - Aging in Phase Change Materials (dots figure)

- Motivation
  - "Amorphous materials are out of thermodynamic equilibrium"
  - subject to physical aging
  - phase-change materials (PCMs) have a fast, reversible switch between a conductive crystalline and more resistive amorphous phase
  - aging increases the resistivity - 'resistance drift'
  - computer simulation to investigate relaxation processes
  - **Modeling comment:** complexity of the chemistry requires DFT to describe and understand bonding and the amorphous phase
- Literature
  - DFT simulations of GeSbTe alloys report many tetrahedrally bonded Ge, which does not exist in crystal. These are obtained from MQ calcs
- Methods
  - Car-Parrinello
  - **To circumvent time scale problem, generated collection of a-structures**
  - mixed Gaussian/plane wave code in CP2K

- cutoff 300 Ry
  - sampled at gamma only
  - annealed using plane-wave code in Quantum Espresso
  - 34 Ry
  - 3.84 fs
  - Berendsen thermostat
  - 10 models produced starting from liquid
- Results
    - $\text{Ge}^T$  is associated with homopolar Ge-Ge bonds
    - heat of formation shows homopolar bonds more favorable in GeTe than GeSe and SnTe
    - wanted to investigate effects of varying amounts Ge-Ge bonds
    - used different alloys along the phase diagram and substituted with Ge or Te to form different GeTe structures "mimicking aging"
    - homopolar bonds correlated with tetrahedral Ge
    - freezing at density of amorphous GeTe, tetrahedral rich models had the largest values of stress
    - this agrees with experiments showing the drift of PCMS is accompanied by stress relief
    - order parameter  $d_4/d_0$  goes from tetrahedrally bonded Ge,  $\text{Ge}^T$ , to  $\text{Ge}^{III}$  and  $d_3/d_0$  goes from  $\text{Te}^{II}$  to  $\text{Te}^{III}$
    - increase in band gap directly linked to decrease in homopolar bonds
    - "melt-quenched model has a smaller band gap and possesses a (localized) mid-gap state"

## References

- [1] J. G. Lee, Computational Materials Science: An Introduction, CRC Press, 2012.
- [2] D. S. Sholl, J. A. Steckel, Density Functional Theory: A Practical Introduction, 2009.
- [3] Y.-J. Zhang, J.-H. Lan, C.-Z. Wang, Q.-Y. Wu, T. Bo, Z.-F. Chai, W.-Q. Shi, Theoretical Investigation on Incorporation and Diffusion Properties of Xe in Uranium Mononitride, The Journal of Physical Chemistry C 119 (11) (2015) 5783–5789. doi:10.1021/jp510219a.  
URL <http://pubs.acs.org/doi/10.1021/jp510219a>
- [4] B. Dorado, M. Freyss, B. Amadon, M. Bertolus, G. Jomard, P. Garcia, Advances in first-principles modelling of point defects in UO<sub>2</sub>: f electron correlations and the issue of local energy minima This, Journal of Physics: Condensed Matter 25 (333201) (2013) 1–13.
- [5] J. Y. Raty, W. Zhang, J. Luckas, C. Chen, R. Mazzarello, C. Bichara, M. Wuttig, Aging mechanisms in amorphous phase-change materials, Nature Communications 6 (7467) (2015) 1–8. doi:10.1038/ncomms8467.  
URL <http://dx.doi.org/10.1038/ncomms8467>
- [6] D. Hohl, R. O. Jones, First-principles molecular-dynamics simulation of liquid and amorphous selenium, Physical Review B 43 (5) (1991) 3856–3870. doi:<https://doi.org/10.1103/PhysRevB.43.3856>.  
URL <https://journals.aps.org/prb/abstract/10.1103/PhysRevB.43.3856>